Prediction of Response to Concurrent Chemoradiotherapy with Temozolomide in Glioblastoma: Application of Immediate Post-Operative Dynamic Susceptibility Contrast and Diffusion-Weighted MR Imaging

Eun Kyoung Lee, MD[1], Seung Hong Choi, MD, PhD[1, 2], Tae Jin Yun, MD[1], Koung Mi Kang, MD[1], Tae Min Kim, MD[3], Se-Hoon Lee, MD[3], Chul-Kee Park, MD[4], Sung-Hye Park, MD[5], Il Han Kim, MD[6]

Departments of [1]Radiology, [4]Neurosurgery, and [5]Pathology, Seoul National University College of Medicine, Seoul 03080, Korea; [2]Center for Nanoparticle Research, Institute for Basic Science, and School of Chemical and Biological Engineering, Seoul National University, Seoul 08826, Korea; Departments of [3]Internal Medicine and [6]Radiation Oncology, Cancer Research Institute, Seoul National University College of Medicine, Seoul 03080, Korea

Objective: To determine whether histogram values of the normalized apparent diffusion coefficient (nADC) and normalized cerebral blood volume (nCBV) maps obtained in contrast-enhancing lesions detected on immediate post-operative MR imaging can be used to predict the patient response to concurrent chemoradiotherapy (CCRT) with temozolomide (TMZ).
Materials and Methods: Twenty-four patients with GBM who had shown measurable contrast enhancement on immediate post-operative MR imaging and had subsequently undergone CCRT with TMZ were retrospectively analyzed. The corresponding histogram parameters of nCBV and nADC maps for measurable contrast-enhancing lesions were calculated. Patient groups with progression (n = 11) and non-progression (n = 13) at one year after the operation were identified, and the histogram parameters were compared between the two groups. Receiver operating characteristic (ROC) analysis was used to determine the best cutoff value for predicting progression. Progression-free survival (PFS) was determined with the Kaplan-Meier method and the log-rank test.
Results: The 99th percentile of the cumulative nCBV histogram (nCBV C99) on immediate post-operative MR imaging was a significant predictor of one-year progression ($p = 0.033$). ROC analysis showed that the best cutoff value for predicting progression after CCRT was 5.537 (sensitivity and specificity were 72.7% and 76.9%, respectively). The patients with an nCBV C99 of < 5.537 had a significantly longer PFS than those with an nCBV C99 of ≥ 5.537 ($p = 0.026$).
Conclusion: The nCBV C99 from the cumulative histogram analysis of the nCBV from immediate post-operative MR imaging may be feasible for predicting glioblastoma response to CCRT with TMZ.
Index terms: *Glioblastoma; Temozolomide; Apparent diffusion coefficient; Cerebral blood volume; Histogram analysis*

INTRODUCTION

Glioblastoma (GBM) is the most common primary brain tumor, representing 12–15% of all intracranial neoplasms and 60–75% of astrocytomas (1). The current standard treatment for GBM is maximally safe tumor resection followed by radiation therapy with concurrent temozolomide (TMZ) and adjuvant TMZ. However, the prognosis is poor,

and the median survival is 14.6 months with radiotherapy plus TMZ (2).

Immediate postoperative radiological imaging is used to assess the residual tumor remaining after surgery and to detect surgical complications as early as possible (3-5). Gadolinium-enhanced MR imaging is extremely valuable for assessing gross residual tumor when performed during days 1 to 3 after the resection of a preoperatively enhancing high-grade glioma. This timing prevents surgically induced contrast enhancement and minimizes interpretative difficulties (5, 6). Many previous studies that used early post-operative MR imaging to evaluate malignant gliomas demonstrated that parenchymal enhancement after contrast media infusion strongly correlates with the presence of residual cancer tissue and is a useful predictive prognostic factor for GBM patient survival (3, 6-9). However, the enhancement pattern itself is known to have limitations in differentiating residual tumors from enhancement caused by postoperative changes (5, 10, 11). Thus, these contrast enhancements are commonly recommended to be evaluated by perfusion-weighted imaging (PWI) or diffusion-weighted imaging (DWI). Dynamic susceptibility contrast (DSC) PWI is a technique that can provide physiologic information such as vascular endothelial proliferation, vascular density, and angiogenesis (12), and DWI can show information about the cellular density and properties of the extracellular matrix. The apparent diffusion coefficient (ADC) calculated from DWI can serve as a marker of cellularity (13).

Although gross-total resection was the preferred procedure, focal residual enhancing lesions after tumor resection have occasionally been noted on immediate post-operative MR imaging. To the best of our knowledge, however, the use of DSC PWI and DWI to predict the patient response to concurrent chemoradiotherapy (CCRT) with TMZ on immediate post-operative MR imaging has not previously been reported. The aim of the present study was to retrospectively evaluate parameters from the histogram analysis of normalized ADC (nADC) and normalized cerebral blood volume (nCBV) maps of measurable enhancing lesions on immediate post-operative MR imaging in patients with GBM who were treated with CCRT with TMZ. We hypothesized that parameters obtained from the histogram analysis of the nADC and nCBV maps could be used to predict the GBM patient response to CCRT with TMZ.

MATERIALS AND METHODS

This retrospective study was approved by the Institutional Review Board of Seoul National University Hospital. The requirement for informed consent was waived.

Patient Selection

Sixty-six patients with GBM who had undergone surgical resection at our institution between June 2009 and September 2012 were selected for this study from our radiology report database of patients with astrocytic tumors. The inclusion criteria were as follows: 1) histopathologic diagnosis of GBM based on the World Health Organization criteria, without oligodendroglial components; 2) immediate post-operative MR imaging performed with DWI and DSC PWI within 24–72 hours after surgery, which was suggested according to the Response Assessment in Neuro-Oncology (RANO) criteria (14); 3) CCRT with TMZ and six cycles of adjuvant TMZ administered after surgical resection; and 4) follow-up contrast-enhanced MR imaging after two to six cycles of adjuvant TMZ.

Forty-two patients were excluded because of the following: 1) extent of surgery, including partial resection and biopsy; 2) inadequate MR images; 3) no visible enhancing lesion at the tumor resection margin in the immediate post-operative MR images; and 4) an enhancing lesion that did not fulfill the criterion of measurable disease, which was defined as a bidimensionally contrast-enhancing lesion with two perpendicular diameters of at least 5 mm.

A total of 24 patients (16 men, 8 women; mean age, 50.1 years; age range, 21–77 years) were included in the present study. The RANO criteria were used to classify the progression and non-progression groups. Based on the RANO criteria, complete response, partial response and stable disease were classified as the non-progression group, and progression was classified as the progression group.

Author gathered the clinical characteristics of each patient, including age, sex, Karnofsky performance status (KPS) score, methylation status of the O^6-methylguanine DNA methyltransferase (MGMT) tumor promoter, preoperative tumor volume, and CCRT radiation dose from the electronic medical records at our institution.

Image Acquisition

For each patient, the immediate post-op MR imaging was performed using 1.5T scanners (n = 6, Signa Excite

1.5T [n = 4]; SignaHDxt 1.5T [n = 2], GE Medical Systems, Milwaukee, WI, USA) or 3T scanners (n = 18, Verio [n = 15]; Siemens Medical Solution, Erlangen, Germany; Signa Excite 3T [n = 3], GE Medical Systems, Milwaukee, WI, USA). The brain imaging sequences included axial spin-echo T1-weighted (T1W) images, fast/turbo spin-echo T2-weighted (T2W) images, fluid-attenuated inversion-recovery images, DWI, DSC-PWI with gadobutrol (Gadovist, Bayer Healthcare, Berlin, Germany), and subsequent contrast-enhanced spin-echo T1WI. DWI was performed with a single-shot spin-echo echo-planar imaging (EPI) sequence in the axial plane before the injection of contrast material with b-values of 0 and 1000 sec/mm^2. DWI was acquired in three orthogonal directions and combined into a trace image. Using these data, ADC maps were calculated on a voxel-by-voxel basis with the software that was incorporated into the MRI unit. For DSC-PWI, a single-shot gradient-echo EPI sequence was used during the intravenous injection of the contrast agent. For each section, 60 images were obtained at intervals equal to the repetition time. After four to five time points, a bolus of gadobutrol at a dose of 0.1 mmol/kg of body weight and a rate of 4 mL/sec was injected with an MR-compatible power injector (Spectris; Medrad, Pittsburgh, PA, USA). The bolus of the contrast material was followed by a 30 mL bolus of saline, which was administered at the same injection rate.

Post-Processing and Histogram Analysis

Histogram analysis was performed using the immediate post-operative MR images acquired within 24–72 hours after surgery. The conventional MR images, ADC maps, and DSC PWI were digitally transferred from the picture archiving and communication system workstation to a personal computer for further analysis. The relative CBV (rCBV) was obtained with a dedicated software package (nordicICE; Nordic Imaging Lab, Bergen, Norway) that applied an established tracer kinetic model to the first-pass data (15, 16). First, realignment was performed to minimize patient motion during the dynamic scans. A gamma-variate function, which approximates the first-pass response as it would appear in the absence of recirculation, was used to fit the 1/T2* curves to reduce the effects of recirculation. To reduce the contrast agent leakage effects, the dynamic curves were mathematically corrected (17). After the elimination of recirculation and leakage of the contrast agent, rCBV was computed with numeric integration of the curve. To minimize variances in rCBV in an individual

patient, the pixel-based rCBV maps were normalized by dividing every rCBV value in a specific section by the rCBV value in the unaffected white matter (18). Co-registrations between the contrast-enhanced (CE) T1WI and the nCBV maps and between the CE T1WI and the ADC maps were performed based on geometric information stored in the respective data sets using a dedicated software package (nordicICE) (19). The differences in slice thickness between images were corrected automatically by re-slicing and co-registration, which were based on the underlying structural images. The nCBV and ADC maps were displayed as color overlays on the CE T1WI.

Two neuroradiologists (with 5 and 9 years of brain MR imaging experience, respectively) who were blinded to the clinical data drew polygonal region of interests (ROIs) in consensus that contained the entire enhancing lesions in each section of the co-registered images. Small or thin-rimmed enhancing lesions that did not fulfill the criteria of measurable disease were not included, and areas of necrosis, hemorrhage, or non-tumor macro-vessels that were evident on the CE T1WI were also excluded from the ROIs. After obtaining the total voxel values of the nCBV of each tumor, histogram analysis was performed as follows. The nCBV histograms were plotted with nCBV on the x-axis with a bin size of 0.1, and the y-axis was expressed as a percentage of the total lesion volume by dividing the frequency in each bin by the total number of analyzed voxels. For further quantitative analysis, cumulative nCBV histograms were obtained from the nCBV histograms in which the cumulative number of observations in all of the bins up to the specified bin was mapped on the y-axis as a percentage. The mean nCBV ± standard deviation was derived from the nCBV histograms. For the cumulative nCBV histograms, the 99th percentile of the histogram (nCBV C99) was derived (the Xth percentile point is the point at which X% of the voxel values that form the histogram are found to the left of the histogram) on the basis of findings in a previous report (20).

To minimize the bias from differences in the MR scanners, nADC was used to define the foci with diffusion restriction in the tumor bed. The nADC of each voxel was defined as the ADC of the voxel divided by the ADC of the normal cerebral white matter, where the ADC of the normal white matter was measured at the contralateral side of the main tumor at the uppermost part of the brain. The nADC histograms were plotted with nADC values on the x-axis with a bin size of 0.1, and the y-axis was expressed as a percentage of the total lesion volume by dividing the

frequency in each bin by the total number of analyzed voxels. For further quantitative analysis, cumulative nADC histograms were obtained from the nADC histograms. The mean nADC ± standard deviation was derived from the nADC histograms. The 5th percentile of the cumulative nADC histograms (nADC C5) was also derived from the histograms (21-23).

Statistical Analysis

All statistical analyses were performed with MedCalc version 12.1.0 (MedCalc Software, Mariakerke, Belgium). The Kolmogorov-Smirnov test was used to determine whether the non-categorical variables of the clinical characteristics and histogram parameters were distributed normally.

Fisher's exact test was used to compare the categorical variables of the clinical characteristics between the true progression and non-progression groups. An unpaired Student's t test was used to compare the non-categorical variables between the groups; the test was used to compare the histogram parameters of progression and non-progression. Receiver operating characteristic (ROC) analysis was used to determine the best cutoff values for the histogram parameters that were significant predictors in

differentiating progression from non-progression. From the ROC curve analysis for the optimum cumulative histogram parameter, the cutoff value with the best sensitivity and specificity was calculated. Kaplan-Meier survival analysis and the log-rank test for group comparison were also performed regarding patient age, KPS score, methylation status of the MGMT promoter, and histogram parameters that showed a difference ($p < 0.05$) between progression and non-progression in the t test, which were dichotomized into two groups. In this analysis, patients were defined as having an event if they had died of tumor progression or had had recurrent tumors. The time was measured from the time of the initial surgery to the time of event or the last follow-up. The results with p values less than 0.05 were considered statistically significant.

RESULTS

Eleven and 13 patients were confirmed to have progression and non-progression, respectively, by the time of one year after the surgery. Among the 11 patients with disease progression, four (36%) were confirmed by pathologic results, and seven (64%) showed radiological

Table 1. Clinical Characteristics

Clinical Characteristic	Progression by 1 Year after Surgery	Non-Progression	P
Total number of patients	n = 11	n = 13	
Age, in years	50.4 ± 15.3	49.9 ± 13.3	0.941*
Sex (%)			1.000†
Male	64 (7 of 11)	69 (9 of 13)	
Female	36 (4 of 11)	31 (4 of 13)	
KPS score (%)			1.000†
≥ 90	91 (10 of 11)	92 (12 of 13)	
< 90	9 (1 of 11)	8 (1 of 13)	
MGMT promoter methylation (+) (%)	55 (6 of 11)	77 (10 of 13)	0.390†
Radiation dose, Gy	56.6 ± 7.7	60.8 ± 0.6	0.101*

*Difference between two groups was evaluated using unpaired Student's t test, †Difference between two groups was evaluated using Fisher's exact test. KPS = Karnofsky performance score, MGMT = O^6-methylguanine DNA methyltransferase

Table 2. Normalized Cerebral Blood Volume (nCBV) and Normalized Apparent Diffusion Coefficient (nADC) Histogram Parameters in Progression and Non-Progression Groups

	Progression by 1 Year after Surgery (n = 11)	Non-Progression (n = 13)	$P^†$
ROI volume	118 ± 101	62 ± 64	0.115
nADC			
C5	0.930 ± 0.154	1.005 ± 0.146	0.239
Mean	1.576 ± 0.364	1.544 ± 0.301	0.814
nCBV			
C99*	7.549 ± 3.557	4.742 ± 1.798	0.033
Mean	2.817 ± 1.769	2.067 ± 1.045	0.211

Values are shown as mean ± standard deviation. ROI volumes are expressed in cubic centimeters. *Significant difference between two groups ($p < 0.05$), †Difference between two groups was evaluated using unpaired Student's t test. ROI = region of interest

progression and aggravation of neurologic status. Preoperative tumor volume was not significantly different between the progression and non-progression groups (33 ± 19 and 49 ± 31, respectively, $p = 0.159$). None of the patients' clinical characteristics, including age, sex, KPS, methylation status of MGMT promoter and radiation dose, were significant predictors of progression or non-progression (Table 1).

Table 2 summarizes the nCBV and nADC histogram parameters between the progression and non-progression groups. The nCBV C99 on immediate post-operative MR imaging was significantly higher in the progression group than in the non-progression group ($p = 0.033$) (Fig. 1), although all other parameters showed no significant

difference between the two groups. ROC analysis of nCBV C99 showed that the best cutoff value for predicting progression after CCRT was 5.537, which had a sensitivity and specificity of 72.7% (8 of 11 patients) and 76.9% (10 of 13), respectively.

The results of the Kaplan-Meier survival analysis with the log-rank test are shown in Figure 2. Significant differences were observed in the progression-free survival (PFS) of the patient group that was dichotomized by the nCBV C99 (cutoff value = 5.537) (hazard ratio = 4.005; $p = 0.026$).

DISCUSSION

The results of the present study suggest that the higher-
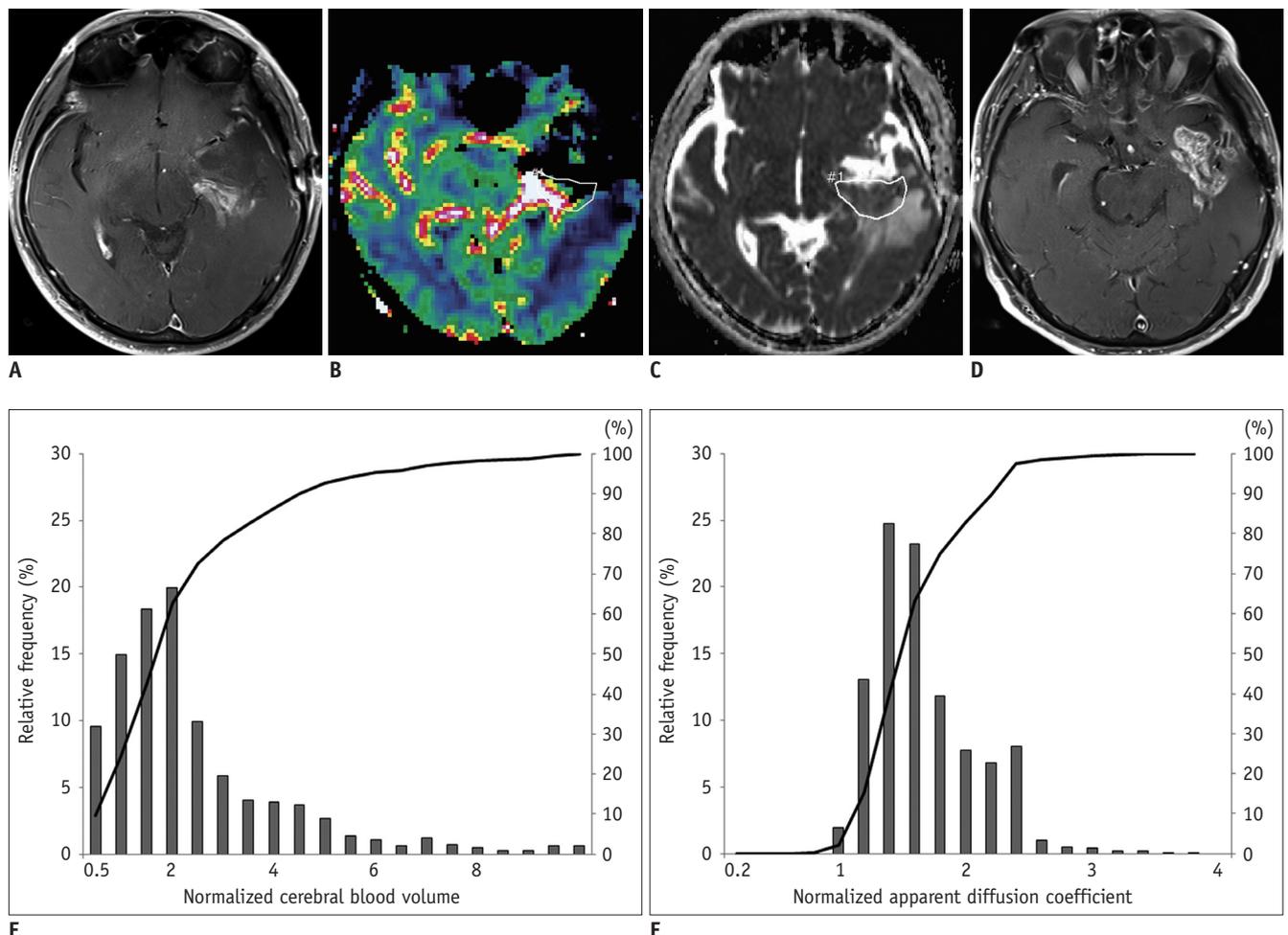
Fig. 1. Representative example of MR images, nCBV maps, nADC maps and corresponding histograms in 70-year-old man with progression and in 60-year-old man with non-progression.
A. Contrast-enhanced T1-weighted MR imaging obtained immediately after gross total resection from 70-year-old man shows measurable enhancement at posterior aspect of tumor resection margin. **B.** nCBV map shows increased nCBV with **(C)** slightly decreased ADC in enhancing lesion. **E.** Normalized CBV histograms and cumulative histograms of enhancing lesion. Histogram for entire contrast-enhancing lesion shows higher frequency of high nCBVs compared with 60-year-old man **(K)**. **F.** Normalized ADC histograms and cumulative histograms of enhancing lesion. **D.** According to follow-up MR images acquired after adjuvant TMZ, there was increase in enhancement of lesion and patients were confirmed as progression. nADC = normalized apparent diffusion coefficient, nCBV = normalized cerebral blood volume, TMZ = temozolomide

end value (C99) of the cumulative nCBV histogram could be used to predict the treatment response after CCRT. However, it is also suggested that other clinical features and MR imaging parameters such as the mean nCBV, mean nADC, and C5 of cumulative nADC histograms could not be used to predict the treatment response. The patients with a low nCBV C99 (C99 < 5.537) had longer PFS compared with the patients with a high nCBV C99 (C99 ≥ 5.537).

The area of contrast enhancement observed on postoperative MR imaging does not always indicate the residual tumor because the contrast enhancement is a reflection of the breakdown of the blood-brain barrier (10, 11). Thus, this study used physiologic parameters from MR imaging such as ADC and CBV to predict the GBM patient response to CCRT with TMZ, and the data suggest that the baseline nCBV C99 can be used to predict whether a patient is likely to have a poor prognosis. A number of previous studies on the application of MR perfusion have shown that rCBV related to progression or survival. Law et al. (12) found that patients who had high-grade gliomas and low-grade gliomas with rCBV of less than 1.75 had significantly longer time to progression than did patients with rCBV of more than 1.75. Similarly, Mangla et al. (24) showed that a decrease in rCBV appears to correlate better with improved survival, but the contrast-enhanced MR imaging–based size criteria do not appear to be as useful. Farace
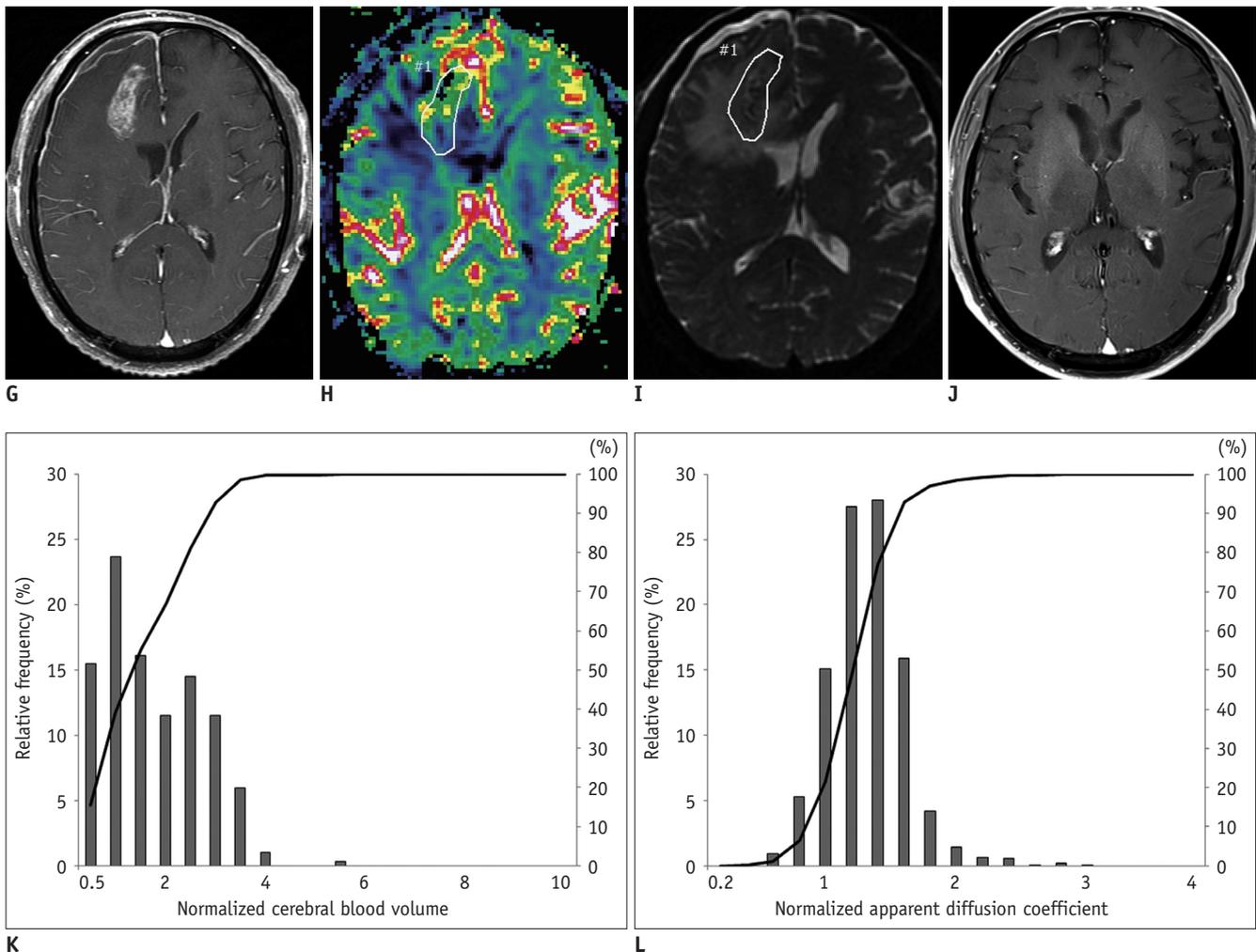
Fig. 1. Representative example of MR images, nCBV maps, nADC maps and corresponding histograms in 70-year-old man with progression and in 60-year-old man with non-progression.
G. Contrast-enhanced T1-weighted MR imaging obtained immediately after gross total resection from 60-year-old man shows measurable enhancement at posteroinferior aspect of tumor resection margin. H. nCBV map shows slightly increased nCBV with (I) slightly decreased ADC in enhancing lesion. K. Normalized CBV histograms and cumulative histograms of enhancing lesion. L. Normalized ADC histograms and cumulative histograms of enhancing lesion. J. According to follow-up MR images acquired after continuing adjuvant TMZ, enhancement of lesion was decreased and patients were confirmed as non-progression. nADC = normalized apparent diffusion coefficient, nCBV = normalized cerebral blood volume, TMZ = temozolomide

et al. (25) compared the early post-operative magnetic resonance (EPMR) images that were acquired within three days of surgery with the pre-adjuvant magnetic resonance (PAMR) images that were acquired approximately one month after surgery. Areas of new contrast enhancement at PAMR were investigated with EPMR DWI and PAMR perfusion imaging. The authors found that areas of increased contrast enhancement with reduced EPMR diffusion often contained postsurgical infarcts and that co-occurrence of hyperperfusion in PAMR perfusion was suggestive of progression. The present study shows that an early increase in the CBV of post-operative enhancing lesions also predicts progression. Thus, we believe that enhancing lesions with a high CBV in immediate post-operative MR imaging should be included in the target delineation for subsequent radiotherapy.

The results of this study showed that the nADC C5 obtained from immediate post-operative MR imaging was not associated with the response of GBM treated with CCRT. ADC changes caused by cystic, necrotic, and/or hemorrhagic areas and the influence of artifacts caused by inhomogeneous structures such as the skull base, bone, and sinus air must be considered. The ADC values from immediate post-operative MR imaging can decrease by postsurgical infarction, hemorrhage, and necrosis (23, 26).

Apart from the intrinsic limits of any retrospective study,

a number of other limitations of the present study should be mentioned. First, this study used a variety of MR imaging scanners with different field strengths (e.g., 1.5T and 3T scanners) from different manufacturers; the scan parameters also differed slightly. Differences in main magnetic field strength and in the scan parameters and processing methodologies of DWIs can bias ADC measurement. A number of recent studies have shown that the ADC values for gray and white matter are significantly lower at 3T compared with 1.5T (27, 28). Huisman et al. (27) suggested that in clinical studies, ADC and fractional anisotropy should be compared with normative values that have been determined for the field strength used. In the present study, ADC was normalized to normal-appearing cerebral white matter in the corona radiata of the contralateral hemisphere to minimize the potential bias. Second, this study included only a small number of patients who met the inclusion criteria, which might have resulted in selection bias. In the present study, recognized prognostic factors such as age, KPS and methylation status of the MGMT promoter showed no significant difference between the two groups. Thus, a future study based on a larger population is warranted regarding this issue. Third, the present study analyzed the correlations between the histogram parameters and PFS only. Overall survival analysis can be affected by some confounders. Overall survival data were not available for a number of patients after disease progression because of lack of follow-up. In addition, many patients underwent hospice care only rather than an ongoing chemotherapeutic plan. Lastly, non-enhancing residual tumor may be present in the operative bed because of the infiltrative nature of high-grade gliomas. In fact, determining the extent of this non-enhancing component of the tumor can be difficult because peritumoral edema has similar radiographic appearances on post-operative MR imaging. Further study is warranted for evaluating the prognosis of non-enhancing lesions on post-operative MR imaging.

In conclusion, the present study suggests that histogram analysis of nCBV maps based on entirely enhancing lesions on immediate post-operative MR imaging may be feasible for predicting treatment response after CCRT in GBM patients.
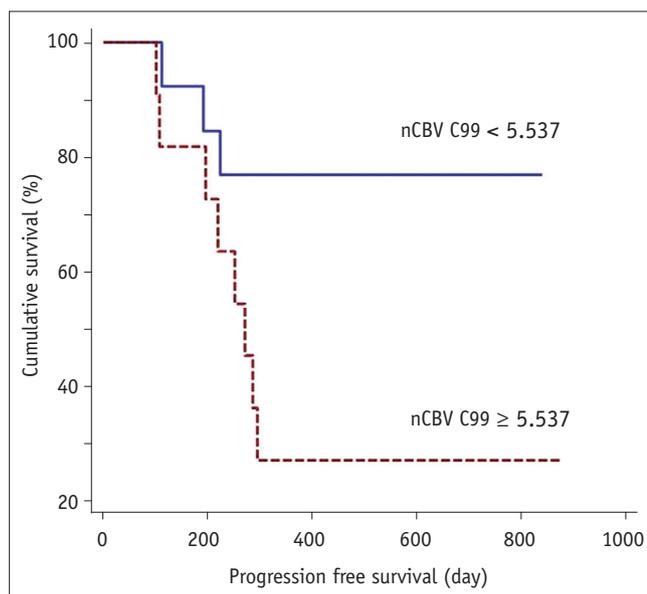
Fig. 2. Kaplan-Meier curves between two groups of patients classified according to cutoff value of 5.537 for C99 of cumulative nCBV histograms (nCBV C99). Significantly better outcomes were noted in group with nCBV C99 less than cutoff value (*p* = 0.026). nCBV = normalized cerebral blood volume

REFERENCES

1. Louis DN, Ohgaki H, Wiestler OD, Cavenee WK, Burger PC, Jouvet A, et al. The 2007 WHO classification of tumours of the

central nervous system. *Acta Neuropathol* 2007;114:97-109

2. Stupp R, Mason WP, van den Bent MJ, Weller M, Fisher B, Taphoorn MJ, et al. Radiotherapy plus concomitant and adjuvant temozolomide for glioblastoma. *N Engl J Med* 2005;352:987-996

3. Ekinci G, Akpinar IN, Baltacıoğlu F, Erzen C, Kiliç T, Elmaci I, et al. Early-postoperative magnetic resonance imaging in glial tumors: prediction of tumor regrowth and recurrence. *Eur J Radiol* 2003;45:99-107

4. Forsyth PA, Petrov E, Mahallati H, Cairncross JG, Brasher P, MacRae ME, et al. Prospective study of postoperative magnetic resonance imaging in patients with malignant gliomas. *J Clin Oncol* 1997;15:2076-2081

5. Henegar MM, Moran CJ, Silbergeld DL. Early postoperative magnetic resonance imaging following nonneoplastic cortical resection. *J Neurosurg* 1996;84:174-179

6. Albert FK, Forsting M, Sartor K, Adams HP, Kunze S. Early postoperative magnetic resonance imaging after resection of malignant glioma: objective evaluation of residual tumor and its influence on regrowth and prognosis. *Neurosurgery* 1994;34:45-60; discussion 60-61

7. Vidiri A, Carapella CM, Pace A, Mirri A, Fabi A, Carosi M, et al. Early post-operative MRI: correlation with progression-free survival and overall survival time in malignant gliomas. *J Exp Clin Cancer Res* 2006;25:177-182

8. Smets T, Lawson TM, Grandin C, Jankovski A, Raftopoulos C. Immediate post-operative MRI suggestive of the site and timing of glioblastoma recurrence after gross total resection: a retrospective longitudinal preliminary study. *Eur Radiol* 2013;23:1467-1477

9. Nakamura H, Murakami R, Hirai T, Kitajima M, Yamashita Y. Can MRI-derived factors predict the survival in glioblastoma patients treated with postoperative chemoradiation therapy? *Acta Radiol* 2013;54:214-220

10. Knopp EA, Cha S, Johnson G, Mazumdar A, Golfinos JG, Zagzag D, et al. Glial neoplasms: dynamic contrast-enhanced T2*-weighted MR imaging. *Radiology* 1999;211:791-798

11. Felix R, Schörner W, Laniado M, Niendorf HP, Claussen C, Fiegler W, et al. Brain tumors: MR imaging with gadolinium-DTPA. *Radiology* 1985;156:681-688

12. Law M, Young RJ, Babb JS, Peccerelli N, Chheang S, Gruber ML, et al. Gliomas: predicting time to progression or survival with cerebral blood volume measurements at dynamic susceptibility-weighted contrast-enhanced perfusion MR imaging. *Radiology* 2008;247:490-498

13. Charles-Edwards EM, deSouza NM. Diffusion-weighted magnetic resonance imaging and its application to cancer. *Cancer Imaging* 2006;6:135-143

14. Wen PY, Macdonald DR, Reardon DA, Cloughesy TF, Sorensen AG, Galanis E, et al. Updated response assessment criteria for high-grade gliomas: response assessment in neuro-oncology working group. *J Clin Oncol* 2010;28:1963-1972

15. Rosen BR, Belliveau JW, Vevea JM, Brady TJ. Perfusion imaging with NMR contrast agents. *Magn Reson Med* 1990;14:249-265

16. Ostergaard L, Weisskoff RM, Chesler DA, Gyldensted C, Rosen BR. High resolution measurement of cerebral blood flow using intravascular tracer bolus passages. Part I: Mathematical approach and statistical analysis. *Magn Reson Med* 1996;36:715-725

17. Boxerman JL, Schmainda KM, Weisskoff RM. Relative cerebral blood volume maps corrected for contrast agent extravasation significantly correlate with glioma tumor grade, whereas uncorrected maps do not. *AJNR Am J Neuroradiol* 2006;27:859-867

18. Wetzel SG, Cha S, Johnson G, Lee P, Law M, Kasow DL, et al. Relative cerebral blood volume measurements in intracranial mass lesions: interobserver and intraobserver reproducibility study. *Radiology* 2002;224:797-803

19. Bjornerud A. The ICE software package: direct co-registration of anatomical and functional datasets using DICOM image geometry information. *Proc Hum Brain Mapping* 2003;19:1018p

20. Kim H, Choi SH, Kim JH, Ryoo I, Kim SC, Yeom JA, et al. Gliomas: application of cumulative histogram analysis of normalized cerebral blood volume on 3 T MRI to tumor grading. *PLoS One* 2013;8:e63462

21. Kang Y, Choi SH, Kim YJ, Kim KG, Sohn CH, Kim JH, et al. Gliomas: Histogram analysis of apparent diffusion coefficient maps with standard- or high-b-value diffusion-weighted MR imaging--correlation with tumor grade. *Radiology* 2011;261:882-890

22. Song YS, Choi SH, Park CK, Yi KS, Lee WJ, Yun TJ, et al. True progression versus pseudoprogression in the treatment of glioblastomas: a comparison study of normalized cerebral blood volume and apparent diffusion coefficient by histogram analysis. *Korean J Radiol* 2013;14:662-772

23. Chu HH, Choi SH, Ryoo I, Kim SC, Yeom JA, Shin H, et al. Differentiation of true progression from pseudoprogression in glioblastoma treated with radiation therapy and concomitant temozolomide: comparison study of standard and high-b-value diffusion-weighted imaging. *Radiology* 2013;269:831-840

24. Mangla R, Singh G, Ziegelitz D, Milano MT, Korones DN, Zhong J, et al. Changes in relative cerebral blood volume 1 month after radiation-temozolomide therapy can help predict overall survival in patients with glioblastoma. *Radiology* 2010;256:575-584

25. Farace P, Amelio D, Ricciardi GK, Zoccatelli G, Magon S, Pizzini F, et al. Early MRI changes in glioblastoma in the period between surgery and adjuvant therapy. *J Neurooncol* 2013;111:177-185

26. Yamasaki F, Sugiyama K, Ohtaki M, Takeshima Y, Abe N, Akiyama Y, et al. Glioblastoma treated with postoperative radio-chemotherapy: prognostic value of apparent diffusion coefficient at MR imaging. *Eur J Radiol* 2010;73:532-537

27. Huisman TA, Loenneker T, Barta G, Bellemann ME, Hennig J, Fischer JE, et al. Quantitative diffusion tensor MR imaging of the brain: field strength related variance of apparent diffusion coefficient (ADC) and fractional anisotropy (FA) scalars. *Eur Radiol* 2006;16:1651-1658

28. Qin W, Yu CS, Zhang F, Du XY, Jiang H, Yan YX, et al. Effects of echo time on diffusion quantification of brain white matter at 1.5 T and 3.0 T. *Magn Reson Med* 2009;61:755-760